

The Strain-Compensated Constitutive Equation for High Temperature Flow Behavior of an Al-Zn-Mg-Cu Alloy

M.R. Rokni, A. Zarei-Hanzaki, C.A. Widener, and P. Changizian

(Submitted February 4, 2014; in revised form July 19, 2014; published online August 12, 2014)

In order to study flow stress behavior for hot working of a typical Al-Zn-Mg-Cu alloy, experimental stress-strain data obtained from isothermal hot compression tests at strain rates of 0.004, 0.04, and 0.4 s⁻¹ and deformation temperatures of 400, 450, 500, and 520 °C were used to develop the constitutive equation. The peak stress decreased with increasing deformation temperature and decreasing strain rate. The effects of temperature and strain rate on deformation behavior were represented by Zener-Hollomon parameter in an exponent-type equation. Employing an Arrhenius-type constitutive equation, the influence of strain has been incorporated by considering the related material constants as functions of strain. The accuracy of the developed constitutive equations has been evaluated using standard statistical parameters such as correlation coefficient and average absolute relative error. The results indicate that the proposed strain-dependent constitutive equation gives an accurate and precise estimate of the flow stress in the relevant temperature range.

Keywords aluminum alloys, compensation of strain and strain rate, constitutive equation, hot compression deformation

1. Introduction

The Al-Zn-Mg-Cu alloy series are very attractive materials to be employed in the automotive and aerospace industries. This is mainly due to their excellent combination of properties such as high strength to weight ratio, fracture toughness, and resistance to stress corrosion cracking (SCC) (Ref 1). Understanding the flow behavior of this alloy in high temperature conditions has a great importance for designers of metal forming processes, and, in turn, many attempts have been made in this regard in the recent years (Ref 1-4). However, the high temperature deformation behavior of metallic materials is always accompanied with various interconnecting metallurgical phenomena such as work hardening, dynamic recovery, dynamic recrystallization, and flow instability (Ref 5-9). In addition, the relationships between the flow stress and these phenomena are nonlinear. Therefore, the modeling and prediction of flow behavior of metallic materials at high temperature is quite challenging. However, the finite element method (FEM) offers a good opportunity to overcome this difficulty (Ref 10). But, the accuracy of such simulations mainly depends on the

accuracy of the deformation flow behavior of the material which is represented by the constitutive equations (Ref 11).

In the previous investigations, various models, such as Johnson-Cook (Ref 12) and Zerilli-Armstrong models (Ref 13), have been proposed to predict the constitutive behavior in a broad range of metals and alloys. However, these exponent-type equations break at low stresses. Jonas et al. (Ref 14) have proposed a phenomenological approach where the flow stress is expressed by the hyperbolic laws in an Arrhenius type of equation. This could track the hot deformation behavior of materials more accurately than the others. Many studies have been performed to assess this equation to suitably applying it to a range of materials (Ref 15-17). However, most of the previous researches have not generally considered the effect of strain, which possesses a critical effect on the accurate prediction of the flow behavior.

In a latter approach, Sloof et al. (Ref 18) introduced a strain-dependent parameter into the sine hyperbolic constitutive equation (also known as Garofalo equation), to predict the flow stress in a wrought magnesium alloy. This revised constitutive equation has been widely used to predict the elevated temperature flow behavior of different steels (Ref 19-21), Al (Ref 22-25), Mg (Ref 9, 18), and Ti (Ref 26, 27) alloys, and even composites (Ref 28). Some authors have also incorporated the compensation of strain rate, in addition to strain compensation, to improve the predictability of the constitutive model (Ref 19). Nevertheless there is a lack of knowledge on the strain-dependent constitutive analysis of Al-Zn-Mg-Cu alloys.

In this paper, isothermal compression of Al-6.09% Zn-2.68% Mg-1.28% Cu alloy, one of the most important heat-treatable aluminum alloys, has been conducted at different temperatures and strain rates to characterize the flow behavior during hot working. Based on the experimental data, a set of constitutive equations relating flow stress, strain rate, and temperature by considering the proper compensation of strain are derived to describe the plastic flow properties. Finally, the

M.R. Rokni and C.A. Widener, Department of Materials & Metallurgical Engineering, Advanced Materials Processing Center, South Dakota School of Mines & Technology (SDSM&T), Rapid City, SD; and A. Zarei-Hanzaki and P. Changizian, School of Metallurgy and Materials Engineering, College of Engineering, University of Tehran, Tehran, Iran. Contact e-mail: mohammadreza.rokni@mines.sdsmt.edu.

Table 1 The chemical composition of the experimental Al-Zn-Mg-Cu Al alloy

Element	Zn	Mg	Cu	Fe	Si	Cr	Ni	Ti	Al
Wt.%	6.09	2.68	1.28	0.18	0.13	0.12	0.01	0.01	Bal.

validity of the developed constitutive equation has been examined for the entire experimental range.

2. Materials and Methods

The experimental aluminum alloy employed in this study was received as-extruded bars, the chemical composition of which is given in Table 1. Figure 1 shows the initial microstructure of the as-received alloy. The cylindrical specimens for uniaxial compression testing were machined from the as-received materials with diameter of 8 mm and height of 12 mm in the extrusion direction in accordance with ASTM E209 (Ref 29). The hot compression tests were carried out with a Gotech-AI7000 servo-controlled electronic universal testing machine equipped with electrical resistance furnace. The load-stroke data were recorded using a high accuracy load cell (Model: SSM-DJM-20 kN) measuring load forces down to 1 kg. Then the load-deformation curve is converted to the engineering stress-strain curve and subsequently to true stress-strain curve. Then the elastic region is removed from the engineering stress-strain curve to get the true stress-plastic strain curve (get a lower absolute average error) (Ref 30). Prior to hot compression, the specimens were soaked at deformation temperature for 7 min to ensure a homogenous temperature distribution. The experimental temperatures were 400, 450, 500, and 520 °C. The reason for considering 520 °C as a last temperature is the presence of liquid phase in the microstructure from the little above this temperature, as it has been already investigated by the authors (Ref 3, 5). At each deformation temperature, the constant strain rates of 0.004, 0.04, and 0.4 s⁻¹ were employed and the specimens were isothermally deformed to true strain of 0.5. A very thin mica plate was used to minimize the friction effect and also to prevent the adhesion of the specimen on the die.

3. Results and Discussion

3.1 Flow Stress Behavior

Figure 2 shows the true stress-true strain curves of the experimental alloy after testing at temperature range of 400–520 °C under the strain rates of 0.004, 0.04, and 0.4 s⁻¹. The influence of temperature and strain rate on the flow stress level is observed in this figure. All the curves, except for 400 and 450 °C at 0.004 s⁻¹, exhibit a peak stress at a certain strain followed by a dynamic flow softening regime up to the end of straining. It should be noted that the aforementioned peaks are more pronounced as the temperature or strain rate increased. Applying higher strain rates can lead to higher rate of dislocation accumulation as well as adiabatic temperature rise, which can increase the extent of softening and accelerate the occurrence of DRX (Ref 31). At 400 and 450 °C with the strain rate of 0.004 s⁻¹, the stress-strain curves show work-hardening and steady-state characteristics, respectively, without any peak

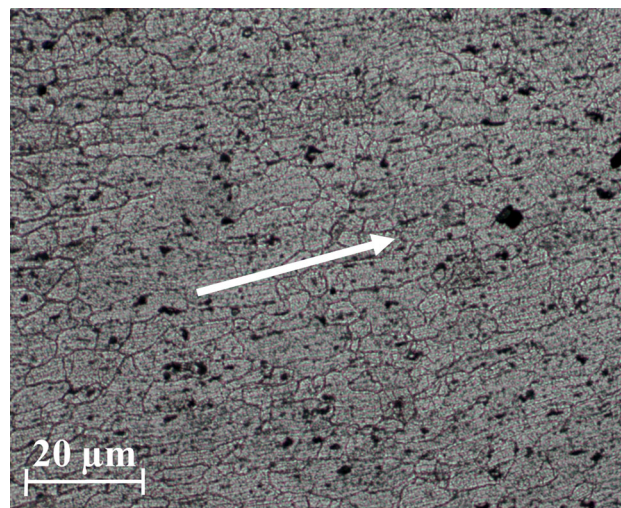


Fig. 1 The optical micrograph of 7075 aluminum alloy in the as-extruded condition. The extrusion direction is indicated with white arrow

stress. It is also evident from the curves that the flow stress level and the peak stress increase with increasing the strain rate and decreasing the deformation temperature. The formation of tangled dislocation structures, as barriers to the dislocation movement, due to the higher strain rates is believed to be the reason for the observed behavior (Ref 3, 32). The presence of more precipitates at lower temperatures in the experimental alloy may also contribute to the increased flow stress level (Ref 3, 5, 32). It appears from inspection of Fig. 2 that the peak strain increases by reducing the deformation temperature and increasing the strain rate. This is rationalized considering the effect of the temperature on restoration processes. Since these processes are thermally activated ones, they are delayed as the deformation temperature decreases (Ref 33). This in turn may shift the peak strain toward higher value. On the other hand, increasing the strain rate would also end to the retardation of softening processes due to the relatively lesser time available for the restoration to be completed. From the aforementioned stress-strain characters, it can be concluded that the work-hardening effect is pronounced at higher strain rate and lower temperature.

3.2 Deformation Constitutive Equations

The Arrhenius equation is widely used to describe the relationship between the strain rate, flow stress, and temperature, especially at high temperatures (Ref 17). Also, the effects of the temperatures and strain rate on the deformation behaviors can be represented by Zener-Hollomon parameter in an exponent-type equation (Ref 34). The hyperbolic law in Arrhenius-type equation gives better approximations between Zener-Hollomon parameter and flow stress. These are mathematically expressed as

$$Z = \dot{\epsilon} \exp\left(\frac{Q}{RT}\right) \quad (\text{Eq 1})$$

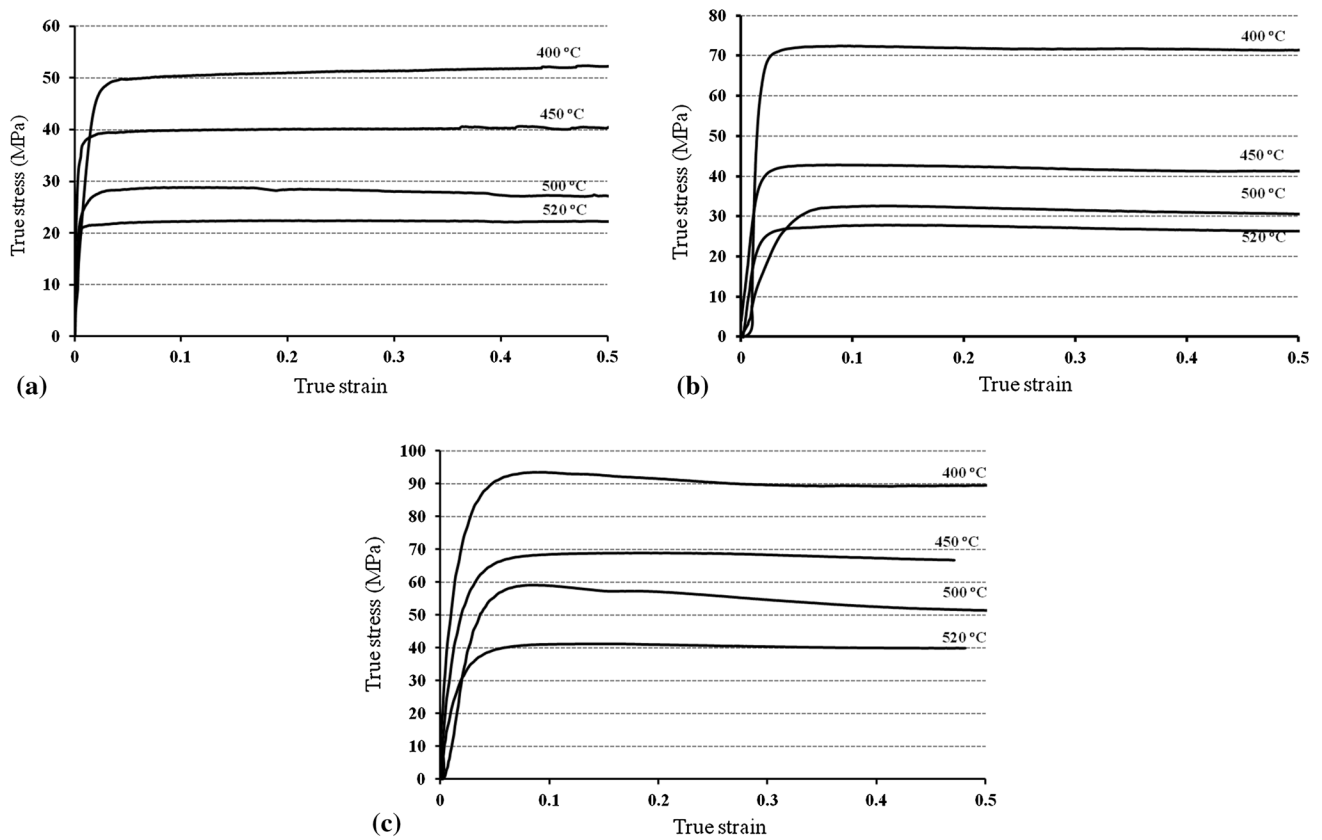


Fig. 2 The true stress-true strain curves of 7075 aluminum alloy during hot compression at the temperature range of 400-520 °C and different strain rates of (a) 0.004 s^{-1} , (b) 0.04 s^{-1} , and (c) 0.4 s^{-1}

$$\dot{\epsilon} = AF(\sigma) \exp\left(\frac{-Q}{RT}\right), \quad (\text{Eq 2})$$

where

$$F(\sigma) = \begin{cases} \sigma^{n_1} & \alpha\sigma < 0.8 \\ \exp(\beta\sigma) & \alpha\sigma > 1.2 \\ [\sinh(\alpha\sigma)]^n & \text{all } \sigma \end{cases} \quad (\text{Eq 3})$$

in which $\dot{\epsilon}$ is the strain rate (s^{-1}), R is the universal gas constant (8.314 J/mol/K); T the absolute temperature (K), σ the flow stress (MPa), Q is the activation energy (kJ/mol); A , β , n_1 , α , and n are the materials constants and experimentally determined temperature-independent. The constant n is the stress exponent and the stress multiplier α is an adjustable constant which brings $\alpha\sigma$ into the correct range to make constant T curves linear and parallel. For the high-stress level, mathematical analyses of the exponential law and the hyperbolic law show that: $\alpha = \beta/n_1$. For the low-stress level, mathematical analyses of the power law and the hyperbolic law show that: $n_1 \sim n$. So α and n can be simply determined from data for high and low stresses. According to Eq 2 and 3, the peak stress (Ref 25, 35) or steady-state stress (Ref 14, 36) can be calculated at a given strain rate and temperature. It is required that the material constants α , n , A , and activation energy Q of the hot forming be known.

3.3 Determination of Materials Constants

To determine the material constants which appear in these equations, the stress-strain data obtained from the compression

tests under different conditions of strain rate and temperature can be used. The evaluation procedure of material constants at true strain of 0.15 as an example is as follows. For low and high-stress levels (at constant temperature), substituting the values of $F(\sigma)$ in Eq 2 gives the following relationships, respectively:

$$\dot{\epsilon} = B\sigma^{n_1} \quad (\text{Eq 4})$$

$$\dot{\epsilon} = C \exp(\beta\sigma), \quad (\text{Eq 5})$$

where B and C are the material constants. Logarithm of both sides of Eq 4 and 5 yields

$$\ln(\sigma) = \frac{1}{n_1} \ln(\dot{\epsilon}) - \frac{1}{n_1} \ln(B) \quad (\text{Eq 6})$$

$$\sigma = \frac{1}{\beta} \ln(\dot{\epsilon}) - \frac{1}{\beta} \ln(C). \quad (\text{Eq 7})$$

Substituting the values of the flow stress and corresponding strain rate under the strain of 0.15 into the logarithm Eq 6 and 7 gives the relationship between the flow stress and strain rate, as shown in Fig. 3. As clearly seen in this figure, the flow stresses obtained from the hot compression tests can be approximated by the group of parallel and straight lines in the hot deformation conditions. The value of n_1 and β is obtained from the mean slope values of $\ln \sigma - \ln \dot{\epsilon}$ plot and $\sigma - \ln \dot{\epsilon}$ plot (Fig. 3) which were found to be 6.407 and 0.13 MPa^{-1} , respectively. This gives the value of $\alpha = \beta/n_1 = 0.0207 \text{ MPa}^{-1}$. This value falls between the different α values which have been frequently used for various

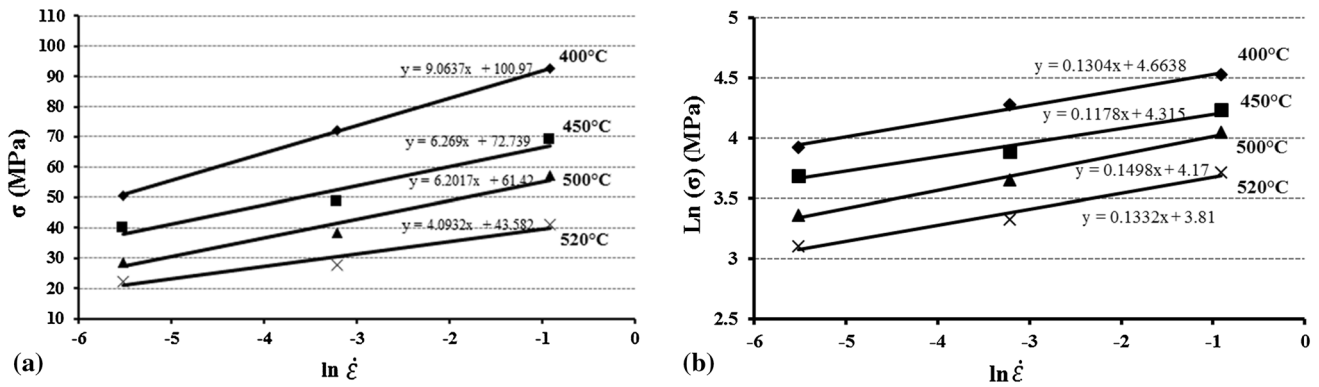


Fig. 3 Evaluating the value of (a) $n1$ by plotting $\ln \sigma$ vs. $\ln \dot{\epsilon}$ and (b) β by plotting σ vs. $\ln \dot{\epsilon}$

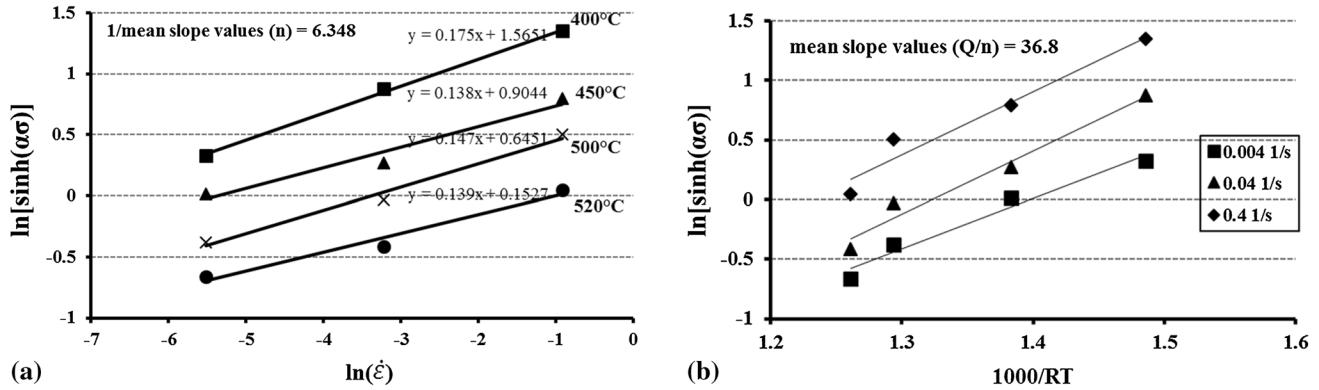


Fig. 4 Evaluating the value of (a) n by plotting $\ln [\sinh(\alpha\sigma)]$ vs. $\ln \dot{\epsilon}$ and (b) Q by plotting $\ln [\sinh(\alpha\sigma)]$ vs. $1000/RT$

7xxx aluminum series containing various amounts of alloying elements (Ref 36-38). For all the strain levels, Eq 2 is rewritten as

$$\dot{\epsilon} = A[\sinh(\alpha\sigma)]^n \exp\left(\frac{-Q}{RT}\right). \quad (\text{Eq 8})$$

Taking the logarithm of both sides of the above equation gives

$$\ln[\sinh(\alpha\sigma)] = \frac{\ln \dot{\epsilon}}{n} + \frac{Q}{(nRT)} - \frac{\ln A}{n}. \quad (\text{Eq 9})$$

From Eq 9, it is clear that at a particular strain, the experimental data should yield linear and parallel lines for different temperatures when $\ln[\sinh(\alpha\sigma)]$ versus $\ln \dot{\epsilon}$ is plotted. This plot at 0.15 strain is shown in Fig. 4(a). For a particular strain (0.15), using the value of α , n was calculated from the average of the slopes of the lines of the same plot. The value of n for the experimental 7075 aluminum alloy is 6.348. This value is in a fair agreement with those previously published for Al-Zn-Mg-Cu alloys (Ref 1, 37).

For calculating hot deformation activation energy (Q) for a particular strain rate differentiating Eq 9 gives

$$Q = Rn \frac{d\{\ln[\sinh(\alpha\sigma)]\}}{d(1/T)}. \quad (\text{Eq 10})$$

Consequently, Q is determined through plotting the variation of stresses at the strain of 0.15 against the reciprocal of absolute temperature. The plot of $\ln(\sinh(\alpha\sigma))$ versus

$1000/RT$ is shown in Fig. 4(b), and the related average slope (Q/n) is about 36.8. The approximate activation energy for deformation in the experimental temperatures (i.e., 233.6 kJ/mol) is extracted by applying the corresponding value of n and presented in Table 2. The calculated activation energy falls between Q values reported for aluminum alloys in the literature (Ref 1, 36, 37). However, it is somewhat higher than that of homogenized 7150 Al alloy (229.75 kJ/mol) (Ref 37), aged 7150 Al alloy (158.8-161.4 kJ/mol) (Ref 35), precipitated and over aged 7012 Al alloy (141-162 kJ/mol) and solution-treated 7012 Al alloy (200-230 kJ/mol) (Ref 1) ones. As it is well known, some deviation in deformation activation energy is acceptable due to the nature of linear regression method used for acquiring the Q value (Ref 16). Furthermore, this difference may be attributed to the concurrence of dynamic precipitation (Ref 39), dislocation pinning effect (Ref 40), and temperature dependence of the solute content (Ref 41).

3.4 Compensation of Strain

It has been recently shown that the strain has a strong influence on the deformation activation energy and material constants (Ref 20-25). Therefore, compensation of strain may have a significant effect on the accuracy of the flow stress prediction and should be taken into account in order to derive the proper constitutive equations. The influence of strain in the constitutive equation is incorporated by assuming that the activation energy (Q) and material constants (i.e., α , n , and

In A) are polynomial function of strains. In the present work, the values of the material constants were evaluated at various strains (in the range of 0.05-0.45) at the intervals of 0.05, the corresponding curves of which are shown in Fig. 5. These values were then employed to fit the polynomial function. A fifth-order polynomial, as shown in Eq 11, was found to represent the influence of strain on the material constants with a very good correlation and generalization. Once the coefficients of these polynomials are determined and replaced in the constitutive equation, the dependency of flow stress to deformation conditions and strain will be evaluated. The coefficients of the polynomial functions are given in Table 3.

$$\alpha = \alpha_0 + \alpha_1 \varepsilon + \alpha_2 \varepsilon^2 + \alpha_3 \varepsilon^3 + \alpha_4 \varepsilon^4 + \alpha_5 \varepsilon^5 \quad (a)$$

$$Q = Q_0 + Q_1 \varepsilon^1 + Q_2 \varepsilon^2 + Q_3 \varepsilon^3 + Q_4 \varepsilon^4 + Q_5 \varepsilon^5 \quad (b)$$

$$n = n_0 + n_1 \varepsilon^1 + n_2 \varepsilon^2 + n_3 \varepsilon^3 + n_4 \varepsilon^4 + n_5 \varepsilon^5 \quad (c)$$

$$\ln A = A_0 + A_1 \varepsilon^1 + A_2 \varepsilon^2 + A_3 \varepsilon^3 + A_4 \varepsilon^4 + A_5 \varepsilon^5 \quad (d)$$

It can be seen that the general trend is an initial decrease in the constant values followed by a later increase at a certain strain (Fig. 5a-d). It is worth to mention that since the α , n , and A are mathematical constants, their variations with strain are not necessarily caused by changes in any microstructural

Table 2 The constants of Al-Zn-Mg-Cu Al alloy used in the hyperbolic sine-type constitutive equation for $\varepsilon = 0.15$

α , MPa ⁻¹	n	Q , kJ/mol
0.0207	6.407	235.78

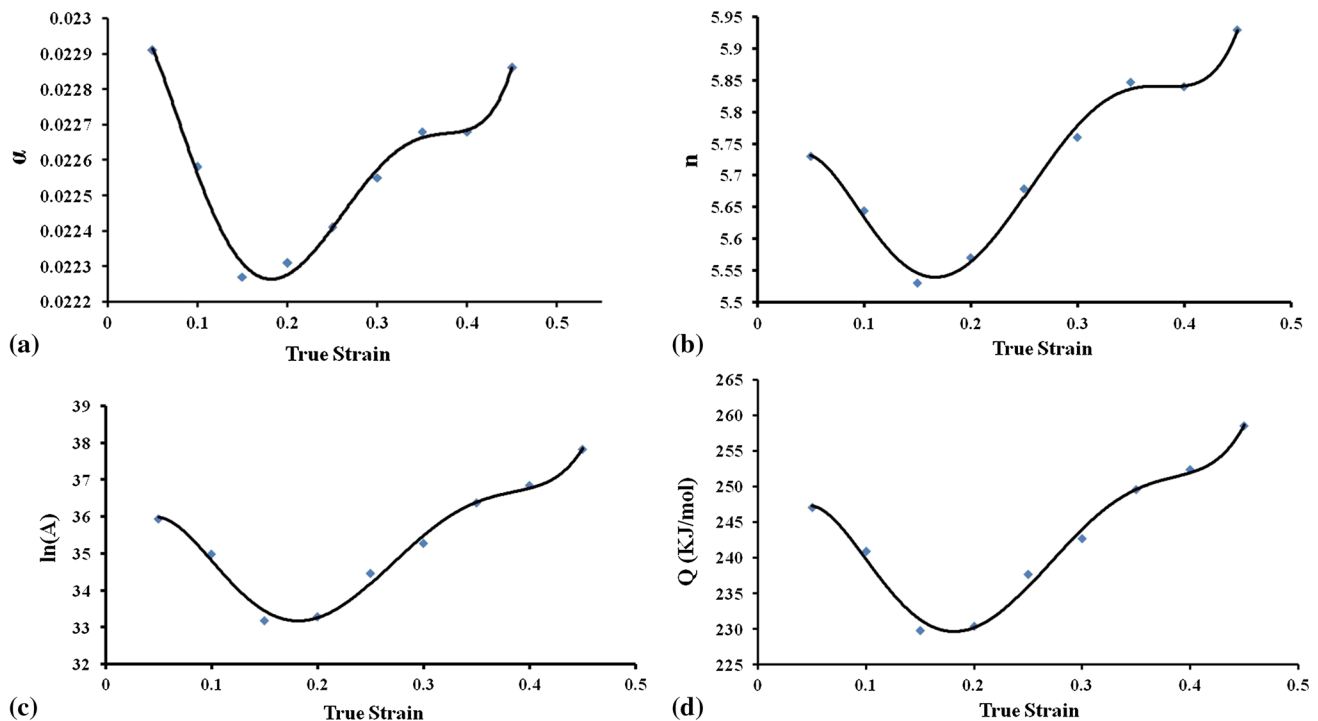


Fig. 5 The variations of (a) α , (b) n , (c) $\ln A$, and (d) Q with true strain along with fifth-order polynomial fit for 7075 aluminum alloy

feature. However, the decay of the activation energy at the beginning of the deformation can be explained by larger vacancies content which is induced by large strain and promotes easier boundary motion (Ref 42, 43). But the reason for the subsequent increase is not clear and it needs further study.

Once the materials constants are evaluated, the flow stress at a particular strain can be predicted. Accordingly, the constitutive equation that relates flow stress and Zener-Hollomon parameter can be written in the following form (considering the Eq 1 and 8):

$$\sigma = \frac{1}{\alpha} \ln \left[\left(\frac{Z}{A} \right)^{1/n} + \left\{ \left(\frac{Z}{A} \right)^{2/n} + 1 \right\}^{1/2} \right]. \quad (\text{Eq 12})$$

3.5 Verification of Constitutive Equation

Figure 6 shows the comparison between the experimental flow curves and those predicted by the developed constitutive equation under different conditions of strain rates and temperatures. As observed from these figures, the predicted flow stress values could well track the experimental data throughout the entire strain range for various testing conditions. However, two processing conditions (i.e., at 400 °C in 0.004 s⁻¹ and 450 °C in 0.04 s⁻¹) show a notable deviation between experimental and predicted flow stress data (Fig. 6b and c). The reason is not quite clear to us. This flow softening can be possibly due to the temperature rise induced by deformation at these deformation conditions (Ref 19). But, then it may be argued here that deformation heating and subsequent flow stress reduction should also take place at other temperatures and strain rates.

Table 3 Coefficients of fifth-order polynomial function for α , Q , n , and A

	α_i coefficient	Q_i coefficient	n_i coefficient	A_i coefficient
$i = 0$	0.023	232.7	5.6	33.6
$i = 1$	0.005	230.2	9.5	120.2
$i = 2$	-0.198	-11,640.0	-151.7	-1897.0
$i = 3$	1.271	63,398.0	871.2	10,298.0
$i = 4$	-3.065	-14,137.0	2024.0	-22,928.0
$i = 5$	2.564	11,241.0	1660.0	18,215.0

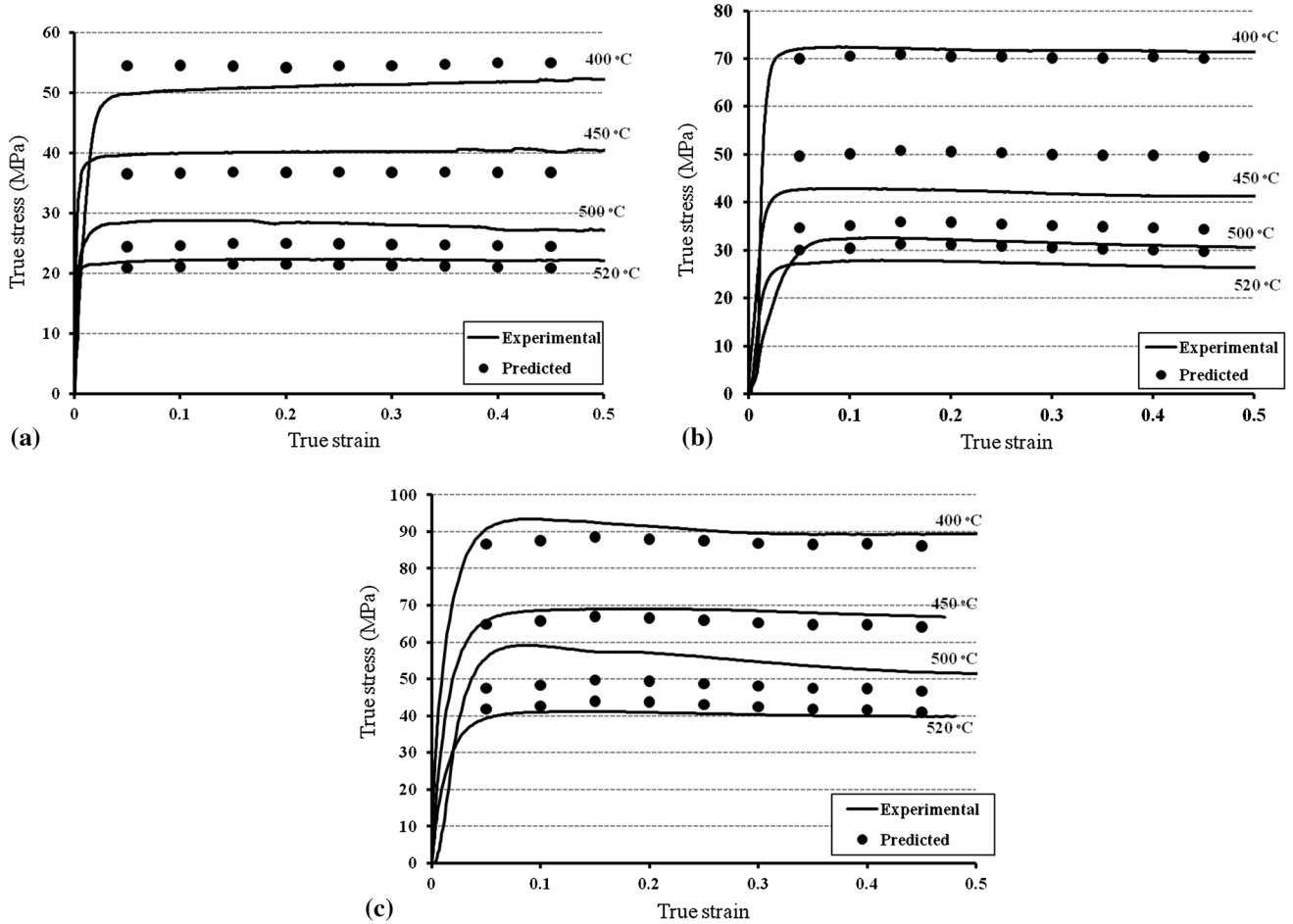


Fig. 6 The comparison of the experimental and predicted flow stress curves for 7075 aluminum alloy compressed at different temperatures and the strain rates of (a) 0.004 s^{-1} , (b) 0.04 s^{-1} , and (c) 0.4 s^{-1}

However, as it can be seen in Fig. 6(b) and (c), the modified equation could predict the flow stress precisely at other conditions. Therefore, a more detailed investigation would need to be conducted before drawing any reliable conclusions.

In order to further evaluation of the predictability of the constitutive equation, the standard statistical parameters such as correlation coefficient (R) and average absolute relative error (AARE), which are expressed through Eq 13 and 14, were employed, respectively.

$$R = \frac{\sum_{i=1}^N (\sigma_{\text{exp}}^i - \bar{\sigma}_{\text{exp}})(\sigma_{\text{p}}^i - \bar{\sigma}_{\text{p}})}{\sqrt{\sum_{i=1}^N (\sigma_{\text{exp}}^i - \bar{\sigma}_{\text{exp}})^2} \sqrt{\sum_{i=1}^N (\sigma_{\text{p}}^i - \bar{\sigma}_{\text{p}})^2}}, \quad (\text{Eq 13})$$

$$\text{AARE} (\%) = \frac{1}{N} \sum_{i=1}^N \left| \frac{\sigma_{\text{exp}}^i - \sigma_{\text{p}}^i}{\sigma_{\text{exp}}^i} \right|, \quad (\text{Eq 14})$$

where σ_{exp}^i is the experimental flow stress, σ_{p}^i is the predicted flow stress, $\bar{\sigma}_{\text{p}}$, and $\bar{\sigma}_{\text{exp}}$ are the mean values of σ_{exp}^i and σ_{p}^i , respectively. The N is the number of data which were employed in the investigation. The correlation coefficient is a commonly used statistical parameter and provides information about the strength of linear relationship between the observed and the calculated values. Sometimes higher value of R may not necessarily indicate a better performance (Ref 19) because of the tendency of the model/equation to be biased toward higher or lower values. The AARE is also computed through

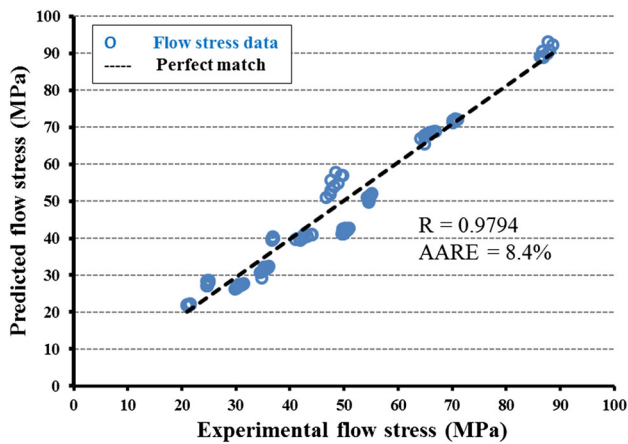


Fig. 7 Correlation between the experimental and predicted flow stress data from the developed constitutive equation

a term-by-term comparison of the relative error and therefore is an unbiased statistical parameter to measure the predictability of a model/equation (Ref 44). In our study, the values of R and AARE were measured to be 0.9794 and 8.4%, respectively (Fig. 7), which reflect proposed deformation constitutive equation can give a reasonable estimation of the flow stress.

4. Conclusions

In the present study, the strain-compensated constitutive behavior of 7075 aluminum alloy was analyzed by performing hot compression tests in the temperature range of 400–520 °C under the strain rates of 0.004, 0.04, and 0.4 s⁻¹. Based on the true stress-strain curves, a revised constitutive equation incorporating the effects of temperature and strain rate was derived by compensation of strain. The influence of strain in the constitutive analysis was incorporated by considering the effect of strain on materials constants (i.e., n , α , Q , and $\ln A$), and a fifth-order polynomial was found to represent these influences with very good correlation. The constitutive equation was found to predict flow stress precisely at strain rates of 0.1 and 1 s⁻¹. However, a significant deviation in the prediction is observed below 0.1 s⁻¹ and above 1 s⁻¹. The breakdown of the constitutive equation at these processing conditions is believed to be due to adiabatic temperature rise during this high strain rate deformation. The predictability of the developed constitutive equation was quantified in terms of correlation coefficient (R) and average absolute relative error (AARE). The R and AARE were measured to be 0.9794 and 8.4%, respectively, which reflect the excellent prediction capability of the developed strain-compensated constitutive equation.

References

- E. Cerri, E. Evangelista, A. Forcelllese, and H.J. McQueen, Comparative Hot Workability of 7012 and 7075 Alloys After Different Pretreatments, *Mater. Sci. Eng. A*, 1995, **197**, p 181–198
- G.Z. Quan, K.W. Liu, J. Zhou, and B. Chen, Dynamic Softening Behaviors of 7075 Aluminum Alloy, *Trans. Nonferrous Met. Soc. China*, 2009, **19**, p 537–541
- M.R. Rokni, A. Zarei-Hanzaki, A.A. Roostaei, and H.R. Abedi, An Investigation into the Hot Deformation Characteristics of 7075 Aluminum Alloy, *Mater. Des.*, 2011, **32**, p 2339–2344
- H.V. Atkinson, K. Burke, and G. Vaneetveld, Recrystallisation in the Semi-solid State in 7075 Aluminium Alloy, *Mater. Sci. Eng. A*, 2008, **490**, p 266–276
- M.R. Rokni, A. Zarei-Hanzaki, H.R. Abedi, and N. Haghdadi, Microstructure Evolution and Mechanical Properties of Backward Thixoextruded 7075 Aluminum Alloy, *Mater. Des.*, 2012, **36**, p 557–563
- M.R. Rokni, A. Zarei-Hanzaki, and H.R. Abedi, Microstructure Evolution and Mechanical Properties of Back Extruded 7075 Aluminum Alloy at Elevated Temperatures, *Mater. Sci. Eng. A*, 2012, **532**, p 593–600
- A. Abolhasani, A. Zarei-Hanzaki, H.R. Abedi, and M.R. Rokni, The Room Temperature Mechanical Properties of Hot Rolled 7075 Aluminum Alloy, *Mater. Des.*, 2012, **34**, p 631–636
- Y.H. Li, D.D. Wei, J.J. Liu, and X.F. Wang, Constitutive Equation to Predict Elevated Temperature Flow Stress of V150 Grade Oil Casing Steel, *Mater. Sci. Eng. A*, 2011, **530**, p 367–372
- P. Changizian, A. Zarei-Hanzaki, and A.A. Roostaei, The High Temperature Flow Behavior Modeling of AZ81 Magnesium Alloy Considering Strain Effects, *Mater. Des.*, 2012, **39**, p 384–389
- S.K. Singh, K. Mahesh, A. Kumar, and M. Swathi, Understanding Formability of Extra-Deep Drawing Steel at Elevated Temperature Using Finite Element Simulation, *Mater. Des.*, 2010, **31**, p 4478–4484
- Y.C. Lin and G. Liu, A New Mathematical Model for Predicting Flow Stress of Typical High-Strength Alloy Steel at Elevated High Temperature, *Comput. Mater. Sci.*, 2010, **48**, p 54–58
- G.R. Johnson and W.H. Cook, A Constitutive Model and Data for Metals Subjected to Large Strains, High Strain Rates and High Temperatures, *Proceedings of Seventh International Symposium on Ballistics*, The Hague, 1983, p 541–547
- F.J. Zerilli and R.W. Armstrong, Dislocation Mechanics Based Constitutive Relations for Material Dynamics Calculations, *J. Appl. Phys.*, 1987, **61**(5), p 1816–1825
- J.J. Jonas, C.M. Sellars, and McG Tegart, Strength and Structure Under Hot-Working Conditions, *Int. Met. Rev.*, 1969, **14**, p 1–24
- Y.C. Lin and X.M. Chen, A Critical Review of Experimental Results and Constitutive Descriptions for Metals and Alloys in hot Working, *Mater. Des.*, 2011, **32**, p 733–759
- M.R. Rokni, A. Zarei-Hanzaki, A.A. Roostaei, and A. Abolhasani, Constitutive Base Analysis of a 7075 Aluminum Alloy During Hot Compression Testing, *Mater. Des.*, 2011, **32**, p 4955–4960
- C.M. Sellars and W.J. McTegart, On the Mechanism of Hot Deformation, *Acta Metall.*, 1996, **14**, p 1136–1138
- F.A. Slooff, J. Zhou, J. Duszczyk, and L. Katgerman, Constitutive Analysis of Wrought Magnesium Alloy Mg-Al4-Zn1, *Scripta Mater.*, 2007, **57**, p 759–762
- S. Mandal, V. Rakesh, P.V. Sivaprasad, S. Venugopal, and K.V. Kasiviswanathan, Constitutive Equations to Predict High-Temperature Flow Stress in a Ti-Modified Austenitic Stainless Steel, *Mater. Sci. Eng. A*, 2009, **500**, p 114–121
- A. Marandi, A. Zarei-Hanzaki, N. Haghdadi, and M. Eskandari, The Prediction of Hot Deformation Behavior in Fe-21Mn-2.5Si-1.5Al Transformation-Twinning Induced Plasticity Steel, *Mater. Sci. Eng. A*, 2012, **554**, p 72–78
- D. Samantaray, S. Mandal, and A.K. Bhaduri, Constitutive Analysis to Predict High-Temperature Flow Stress in Modified 9Cr-1Mo (P91) Steel, *Mater. Des.*, 2010, **31**, p 981–984
- N. Haghdadi, A. Zarei-Hanzaki, and H.R. Abedi, The Effect of Thermomechanical Parameters on the Eutectic Silicon Characteristics in a Non-modified Cast A356 Aluminum Alloy, *Mater. Sci. Eng. A*, 2012, **535**, p 252–257
- Y.C. Lin, Y.C. Xia, X.M. Chen, and M.S. Chen, Constitutive Descriptions for Hot Compressed 2124-T851 Aluminum Alloy Over a Wide Range of Temperature and Strain Rate, *Comput. Mater. Sci.*, 2010, **50**, p 227–233
- L. Ou, Y. Nie, and Z. Zheng, Strain Compensation of the Constitutive Equation for High Temperature Flow Stress of a Al-Cu-Li Alloy, *J. Mater. Eng. Perform.*, 2014, **23**, p 25–30
- H.J. McQueen, E. Fry, and J. Belling, Comparative Constitutive Constants for Hot Working of Al-4.4Mg-0.7 Mn (AA5083), *J. Mater. Eng. Perform.*, 2001, **10**(2), p 164–172

26. M. Li, S. Cheng, A. Xiong, H. Wang, S. Shaobo, and L. Sun, Acquiring a Novel Constitutive Equation of a TC6 Alloy at High-Temperature Deformation, *J. Mater. Eng. Perform.*, 2005, **14**, p 263–266
27. X. Li, M. Li, D. Zhu, and A. Xiong, Deformation Behavior of TC6 Alloy in Isothermal Forging, *J. Mater. Eng. Perform.*, 2005, **14**, p 671–676
28. Y. Yang, F. Li, Z. Yuan, and H. Qiao, A Modified Constitutive Equation for Aluminum Alloy Reinforced by Silicon Carbide Particles at Elevated Temperature, *J. Mater. Eng. Perform.*, 2013, **22**, p 2641–2655
29. ASTM E209, *Standard Practice for Compression Tests of Metallic Materials at Elevated Temperatures with Conventional or Rapid Heating Rates and Strain Rates*, Annual Book of ASTM Standards, ASTM, West Conshohocken, 2010
30. D. Samantaray, S. Mandal, and A.K. Bhaduri, A Critical Comparison of Various Data Processing Methods in Simple Uniaxial Compression Testing, *Mater. Des.*, 2011, **32**, p 2797–2802
31. S. Mandal, A.K. Bhaduri, and V. Subramanya Sarma, Role of Twinning on Dynamic Recrystallization and Microstructure During Moderate to High Strain Rate Hot Deformation of a Ti-Modified Austenitic Stainless Steel, *Metall. Mater. Trans. A*, 2012, **43**, p 2056–2068
32. F.J. Humphreys and M. Hatherly, *Recrystallization and Related Annealing Phenomena*, 2nd ed., Pergamon Press, Oxford, 2004
33. S. Mandal, A.K. Bhaduri, and V. Subramanya Sarma, A Study on Microstructural Evolution and Dynamic Recrystallization During Isothermal Deformation of a Ti-Modified Austenitic Stainless Steel, *Metall. Mater. Trans. A*, 2011, **42**, p 1062–1072
34. C. Zener and H. Hollomon, Effect of Strain Rate Upon Plastic Flow of Steel, *J. Appl. Phys.*, 1994, **15**, p 22–32
35. T. Sheppard and A. Jackson, Constitutive Equations for Use in Prediction of Flow Stress During Extrusion of Aluminium Alloys, *Mater. Sci. Technol.*, 1997, **13**, p 203–207
36. H.J. McQueen and N.D. Ryan, Constitutive Analysis in Hot Working, *Mater. Sci. Eng. A*, 2002, **322**, p 43–63
37. N. Jin, H. Zhang, Y. Han, W. Wu, and J. Chen, Hot Deformation Behavior of 7150 aluminum Alloy During Compression at Elevated Temperature, *Mater. Charact.*, 2009, **60**, p 530–536
38. H.E. Hu, L. Zhen, L. Yang, W.Z. Shao, and B.Y. Zhang, Deformation Behavior and Microstructure Evolution of 7050 Aluminum Alloy During High Temperature Deformation, *Mater. Sci. Eng. A*, 2008, **488**, p 64–71
39. H.J. McQueen, W. Blum, and T. Sato, Ed., *Aluminium Alloys, Physical and Mechanical Properties*, ICAA6, Japan Institute of Metals, Sendai, 1998, p 99–112
40. X. Huang, H. Zhang, Y. Han, and W. Wu, Hot Deformation Behavior of 2026 Aluminum Alloy During Compression at Elevated Temperature, *Mater. Sci. Eng. A*, 2010, **527**, p 485–490
41. J. Van de Langkruis, W.H. Kool, and S. Van der Zwaag, Assessment of Constitutive Equations in Modelling the Hot Deformability of Some Overaged Al-Mg-Si Alloys with varying Solute Contents, *Mater. Sci. Eng. A*, 1999, **266**, p 135–145
42. T. Ungar, E. Schaffler, P. Hanak, S. Bernstorff, and M. Zehetbauer, Vacancy Production During Plastic Deformation in Copper Determined by In Situ X-ray Diffraction, *Mater. Sci. Eng. A*, 2007, **462**, p 398–401
43. Z. Zeng, S. Jonsson, and Y. Zhang, Constitutive Equations for Pure Titanium at Elevated Temperatures, *Mater. Sci. Eng. A*, 2009, **505**, p 116–119
44. D. Samantaray, S. Mandal, and A.K. Bhaduri, A Comparative Study on Johnson Cook, Modified Zerilli-Armstrong and Arrhenius-type Constitutive Models to Predict Elevated Temperature Flow Behaviour in Modified 9Cr-1Mo Steel, *Comput. Mater. Sci.*, 2009, **47**, p 568–576